IEEE Access
Multidisciplinary | Rapid Review | Open Access Journal

Received July 21, 2020, accepted August 6, 2020, date of publication August 11, 2020, date of current version August 21, 2020.

Digital Object Identifier 10.1109/ACCESS.2020.3015865

Bounded Orbits and Multiple Scroll Coexisting Attractors in a Dual System of Chua System

YUE LIU[1,2], (Member, IEEE), HERBERT HO-CHING IU[2], (Senior Member, IEEE), HUI LI[1], AND XUEFENG ZHANG[1]

[1]College of Electrical and Electronic Engineering, Changchun University of Technology, Changchun 130012, China
[2]School of Electrical, Electronic and Computer Engineering, The University of Western Australia, Perth, WA 6009, Australia

Corresponding author: Yue Liu (lycn81@163.com)

This work was supported by the China Scholarship Council (CSC).

ABSTRACT A special three-dimensional chaotic system was proposed in 2016, as a dual system of Chua system, which is satisfied $a_{12}{\cdot}a_{21} < 0$. The dynamics characteristics are different from the Jerk system ($a_{12}{\cdot}a_{21} = 0$) and Chua system ($a_{12}{\cdot}a_{21} > 0$). In this paper, a method for generating $M \times N \times L$ grid multiple scroll attractors is presented for this system. Also, in order to ensure the rigor of the theoretical results, we prove existence of the complex scenario of bounded orbits, such as homoclinic and heteroclinic orbits, and illustrate concurrent created and annihilated of symmetric orbits. Then, Shilnikov bifurcation and the possible relationship between the birth and death of the scroll attractors are studied. Furthermore, two theorems are demonstrated for these bounded orbits. Finally, the Lyapunov exponents, bifurcation diagrams, and multiple scroll coexisting attractors are displayed, which are related to the parameters and initial condition.

INDEX TERMS Grid multiple scroll attractors, homoclinic and heteroclinic orbits, Shilnikov bifurcation, coexisting attractors.

I. INTRODUCTION

By and large, the research on chaos, various types of strange attractors, coexisting attractors, synchronization control and their applications have became the hotspots [1]–[5]. Their interesting and complex dynamical phenomena are applied in various fields, for example chaos prediction in nonlinear viscoelastic plates [6], nonlinear resonances and multi-stability in simple neural circuits [7], synchronization control [8], [33], grid multi-scroll chaotic attractors [4], [5], [9], [30], multi-wing hyper chaotic system [10, 30], electronic circuits [11], [13], [22], [24], image encryption application [25, 34], oscillator of memory elements [14], [35], [36], [41], embedded implementation for digital systems [37]–[40] *et al*. As well as we known, the chaotic application in electronic circuits began Chua circuit and generation of multiple scroll attractors started from Suykens and Vandewalle, beyond the double scroll [1]. Up to now, the main work and research on chaos theory, analysis methods and application fields are as follows: (i) chaotic systems and scroll attractors seem to have reached their maturity, *i.e.* some scholars and their co-workers proposed plenty of methods for designing the grid multi-scroll and multi-wing chaotic and hyper chaotic attractors [4], [5], [9], [29]–[31], L. Zhou and his fellows proposed a novel no-equilibrium hyper chaotic system [10], J. Kengne *et al*. presented dynamics for Jerk or Jerk-like system with multiple attractors [11], [12], [19], Q. Lai and S. Chen proposed a polynomial function method for generating multiple strange attractors from the Sprott B system [31], just to name a few; (ii) all kinds of analysis methods have been described on unusual and striking dynamics, such as the, self-excited antimonotonicity [11], [14], [21] and hidden attractors [15], coexisting attractors [16]–[19], [22]–[24], without equilibrium chaotic system [10], [18], [19], and multiple stability [20] and synchronization [8], [33] as new research directions, are still in their infancy. Especially, in n-scroll chaotic system, the occurrence of two or more asymptotically stable or attracting basin have been analyzed, symmetry and broken symmetry have been reported. For example, J. Kengne and co-workers proposed a novel memristor-based oscillator and analysis chaos, periodic windows, antimonotonicity and crises [11]; Subsequently, the fellows of the this research group, Z.T. Njitacke and co-workers found a autonomous Jerk circuit

The associate editor coordinating the review of this manuscript and approving it for publication was Cihun-Siyong Gong.

and similar prosperities [12]; L. Zhou and his coworkers observed coexisting attractors and antimonotonicity (named the full Feigenbaum tree) in a flux-controlled memristor [14]; Lai Q *et al*. proposed a new 4D chaotic system [17], and represented coexisting attractors [22]–[24], dynamic analysis and circuit realization [31], [32]; In coupled systems, multi-stability of infinitely many attractors was also recently reported [7], [20], and so on; (iii) chaotic applications also became interesting and rich. For example, chaos prediction in nonlinear system subjected to subsonic flow and external load was demonstrated by D. Younesian and H. Norouzi [6], chaotic system synchronization and message recovery scheme was proposed by V. Sharma, B.B. Sharma, and R. Nath [8], [33], the new chaotic systems and their electronic implementation were proposed [13], [21]–[24], image encryp- tion based on some chaotic systems were explored [23]–[25], design and implementation based on the ARM-embedded and FPGA for secure video communication system were presented [37]–[40], and so on; (iv) the proof for existence on the complex scenario of bounded orbits [26]–[29] for chaotic and hyper-chaotic systems are in its infancy. It has became a serious attempt and gained a wide attention in academic circles.

In three-dimensional chaotic systems, for the linear part, $A = [a_{ij}]_{3\times3}$ $(i,j = 1,2,3)$, the most famous Chua system satisfies the condition $a_{12}\cdot a_{21} > 0$ while Jerk system satisfies $a_{12}\cdot a_{21} = 0$. There are many literatures on analysis and applications for some classical chaotic systems, *i.e.* Chua system, Jerk circuit, Van der Pol-Duffing circuit and Sprott B system [3]–[5], [12], [15], [16], [19], [21], *et al*. However, some essential works have been neglected, such as the dual system of Chua system, which is also a special type of a canonical form and proposed in 2016. This system satisfies the condition $a_{12}\cdot a_{21} < 0$. Compared with Chua system and Jerk circuit, it has similar but topologically not equivalent dynamic characteristics [5]. As already noted above, for the sake of the completeness and ensure the characteristics for this type of chaotic system, our motivation is focus on exploring a novel method for generating $M \times N \times L$ multiple grid scroll attractors. Also, the proof on existence of the complex scenario of bounded orbits (such as homoclinic and heteroclinic orbits). Furthermore, analysis the more complex and unusual dynamics for the proposed chaotic system. By a new perspective discusses the relationship between the birth and death of the attractors and the mechanism of chaos (*i.e.* bifurcation, grid scroll attractors and coexisting attractors). This paper is developed in the following sections: the background on the proposed dual system of Chua system is introduced and a novel method for generating $M \times N \times L$ grid multiple scroll attractors is proposed in Section II; the existence of the complex scenario of bounded orbits (*i.e.* homoclinic and heteroclinic orbits) according to Shilnikov Theorem are proved and two theorems are presented for these bounded orbits in Section III; in Secion IV, we also display the domains of parameters space by bifurcation and coexisting scroll attractors; finally, the paper is summarized in Section V.

II. THE THREE-DIMENSIONAL CHAOTIC SYSTEM AND M × N × L GRID MULTIPLE SCROLL ATTRACTORS

A. BACKGROUND

In 2016, we proposed a dual system of Chua system, which can be thought a systematic methodology for creating multiple scroll chaotic attractors from a simple three- dimensional system. One of the simplest and dimensionless form is described as follows:

$$\begin{cases} \dfrac{dx}{dt} = -ay \\ \dfrac{dy}{dt} = x + by - f\,(x+z) \\ \dfrac{dz}{dt} = dx - cz - (d-c)f\,(x+z) \end{cases} \tag{1}$$

where x, y, z are state variables; a, b, c, d are real parameters and $f(x + z)$ is the nonlinear function, which is the method for constructing $2N+1$-and $2(N+1)$-scrolls, as shown at the bottom of the next page, where N, an integer, is the sum of the upper bound. The grid scroll attractors can be displayed simultaneously, as shown in Fig.1.

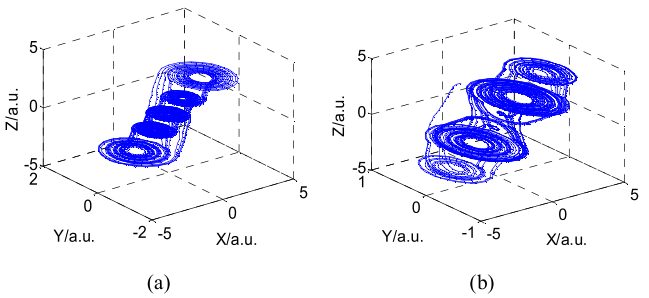

FIGURE 1. The grid multiple scroll chaotic attractors: (a) a = 4, b = 0.2, c = 5, d = 0, N = 2 and initial conditions (0.1, 0.1, 0.1), 5-scroll; (b) a = 9, b = 0.32, c = 5.5, d = 0, N = 2 and initial conditions (0.9, 0.9, 0.9), 6-scroll.

It can be seen that generation of scroll attractors are only along a certain direction, that is $|x+z| = 1$. It is an essential question that whether there are some other methods can obtain multiple scroll attractors along the different directions. In the next subsection, a new way to introduce $M \times N \times L$ grid multiple attractors.

As a simple case of three-dimensional chaotic system (1), which has some insufficient, such as: (i) although the emergence of chaos can be very convincing from computer simulations in this system, there are remain legitimate objections from some critics who demand no less than a rigorous mathematical proof; (ii) according to these parameters, they are not enough to reflect all the complex dynamic characteristics and more details should be required for this type of chaotic systems ($a_{12}\cdot a_{21} < 0$); (iii) especially, the parameter d represents the different feature from the other parameters, that is the horizontal direction of the attractors: if $d = 0$, which means they parallel to the X-axis in horizontal direction; if $d < 0$, which means the horizontal direction and X-axis at obtuse angle; and if $d > 0$, which means the horizontal direction and X-axis at acute angle [5]; (şv) the $f(x + z)$ is the key factor to influence the distribution of grid multiple

scroll attractors. In system (1), the attractors are only in one direction, the others directions cannot be realized; (v) as the dual model of Chua system and a new type of canonical form, the distribution of multiple scroll attractors should be throughout the whole real space. Thus, such a novel method for generating $M \times N \times L$ grid scroll attractors and the existence proof on bounded orbits should be supplied, which are our main objective. Furthermore, the related research on multiple scroll coexisting attractors has been found in no literature before, except [21].

B. THE MODEL AND NOVEL METHOD FOR M × N × L SCROLL ATTRACTORS

Here, the general mathematical model ($a_{12} \cdot a_{21} < 0$) for generating $M \times N \times L$ grid multiple attractors is described as following

$$\begin{cases} \dfrac{dx}{dt} = -e\left[x - f\left(x\right)\right] - a\left[y - f\left(y\right)\right] \\ \dfrac{dy}{dt} = h\left[x - f\left(x\right)\right] + b\left[y - f(y)\right] \\ \dfrac{dz}{dt} = d\left[x - f\left(x\right)\right] - c\left[z - f\left(z\right)\right] \end{cases} \tag{3a}$$

where x, y, z are state variables; a, b, c, d, e, h are real parameters and $f(x)$, $f(y)$, $f(z)$ are the nonlinear *sign* function. It is notice that the *sign* function and five parameters (a, b, c, e, h) are necessary conditions for influencing the location and numbers of scroll attractors, the parameters d also represents the horizontal direction of the attractors. Next, the five main bifurcation parameters are analyzed in detail.

When $M \epsilon R$, $N \epsilon R$, $L \epsilon R$ are three integers, the nonlinear function $f(x)/f(y)/f(z)$ represents the novel methods and $M \times N \times L$ (named three directions) grid multiple scroll attractors, which can be given:

$$f(x) = \begin{cases} A\mathrm{sgn}(x) + A\displaystyle\sum_{n=1}^{N}\begin{bmatrix} \mathrm{sgn}\left(x + 2nA\right) \\ +\mathrm{sgn}\left(x - 2nA\right) \end{bmatrix} & 2N + 1 - Scroll \\ A\displaystyle\sum_{n=1}^{N}\left\{\begin{matrix} \mathrm{sgn}\left[x + (2n-1)A\right] \\ +\left[x - (2n-1)A\right] \end{matrix}\right\} & 2(N+1) - Scroll \end{cases} \tag{3b}$$

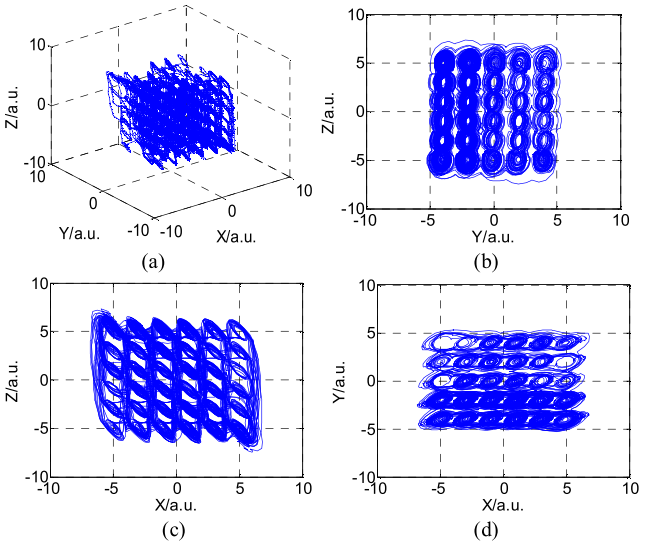

FIGURE 2. 6 × 5 × 6 scroll attractors: (a) 3D; (b) y-z; (c) x-z; (d) x-y.

When $A = 1$, $a = 2$, $b = 0.85$, $c = 0.6$, $d = 1.5$, $e = 0.6$, $h = 0.1$, initial conditions $(0.12, 0.12, 0.12)$, we rewritten the system (3) and $6 \times 5 \times 6$ scrolls can be shown in Fig.2.

$$\begin{cases} \dfrac{dx}{dt} = -0.6 \times \begin{bmatrix} x - \mathrm{sgn}\left(x+1\right) - \mathrm{sgn}\left(x-1\right) \\ -\mathrm{sgn}\left(x+3\right) - \mathrm{sgn}\left(x-3\right) \end{bmatrix} \\ -2 \times \begin{bmatrix} y - \mathrm{sgn}\left(y\right) - \mathrm{sgn}\left(y+2\right) - \mathrm{sgn}\left(y-2\right) \\ -\mathrm{sgn}\left(y+4\right) - \mathrm{sgn}\left(y-4\right) \end{bmatrix} \\ \dfrac{dy}{dt} = 0.1 \times \begin{bmatrix} x - \mathrm{sgn}\left(x+1\right) - \mathrm{sgn}\left(x-1\right) \\ -\mathrm{sgn}\left(x+3\right) - \mathrm{sgn}\left(x-3\right) \end{bmatrix} \\ +0.85 \times \begin{bmatrix} y - \mathrm{sgn}\left(y\right) - \mathrm{sgn}\left(y+2\right) - \mathrm{sgn}\left(y-2\right) \\ -\mathrm{sgn}\left(y+4\right) - \mathrm{sgn}\left(y-4\right) \end{bmatrix} \\ \dfrac{dz}{dt} = 1.5 \times \begin{bmatrix} x - \mathrm{sgn}\left(x+1\right) - \mathrm{sgn}\left(x-1\right) \\ -\mathrm{sgn}\left(x+3\right) - \mathrm{sgn}\left(x-3\right) \end{bmatrix} \\ -0.6 \times \begin{bmatrix} z - \mathrm{sgn}\left(z+1\right) - \mathrm{sgn}\left(z-1\right) \\ -\mathrm{sgn}\left(z+3\right) - \mathrm{sgn}\left(z-3\right) \end{bmatrix} \end{cases} \tag{4}$$

Notably that it is difficult to obtain the same results as the proposed method (*i.e.* nonlinear *sign* function) due to the particularity of system (3), when we choose the other

$$f(x+z) = \begin{cases} \dfrac{1}{2}\displaystyle\sum_{n=1}^{N}\left[\mathrm{sgn}\left(x+z+1\right) + \mathrm{sgn}\left(x+z-1\right)\right] \\ \quad + \dfrac{1}{2}\displaystyle\sum_{n=2}^{N}\left\{\dfrac{2k}{2k-1}\begin{bmatrix} \mathrm{sgn}\left((x+z) + (2k-1)\right) \\ +\mathrm{sgn}\left((x+z) - (2k-1)\right) \end{bmatrix}\right\} & 2N + 1 - Scroll \\ \mathrm{sgn}\left(x+z\right) + \dfrac{1}{2}\displaystyle\sum_{n=1}^{N}\left[\mathrm{sgn}\left(x+z+1\right) + \mathrm{sgn}\left(x+z-1\right)\right] \\ \quad + \dfrac{1}{2}\displaystyle\sum_{n=2}^{N}\left\{\dfrac{2k}{2k-1}\begin{bmatrix} \mathrm{sgn}\left((x+z) + (2k-1)\right) \\ +\mathrm{sgn}\left((x+z) - (2k-1)\right) \end{bmatrix}\right\} & 2(N+1) - Scroll \end{cases} \tag{2}$$

methods (*i.e.* sine function, piecewise function, hyperbolic function *et al.*). Also, this method can be easily implemented by the circuit. Then, it is enough to reflect all the complex dynamic characteristics of this type of chaotic systems and more details can be represented. We have done a lot of experiments to verify it. The most important is that the proposed method is related to prove existence of the complex scenario of bounded orbits and the geometric structure.

It can be obviously observed that the symmetry about the origin ($P_0(0,0,0)$) is shown in system (3). It means that if (x, y, z) is a solution and $(-x,-y,-z)$ is also a solution. Also, the equilibrium points are including $P_0(0,0,0)$, which is a trivial symmetric static solution, and many symmetric nonzero equilibriums $P_{\pm}$. Thus, multiple scroll attractors in phase space are symmetric and occur in pairs. This symmetry may be explain the existence of coexisting scroll attractors in state space. The symmetric equilibrium points, eigenvalues and eigenvectors are shown in Table1.

TABLE 1. Numbers, equilibrium, eigenvalues and corresponding eigenvectors of scroll attractors.

M/ N/ L	$f(x)$	Number	Equilibriums	Eigenvalues and corresponding eigenvectors
0/0/0	-	1	$(0,0,0)$	λ_1= -0.6, λ_2= -0.125 + 0.1561i, λ_3= -0.125 - 0.1561i;
1/1/1	$f_1(x)$/ $f_1(y)$/ $f_1(z)$	3×3×3	(-1-1,-1), (-1,-1,0), ..., (1,1,0), (1,1,1)	ξ_1=[0, 0, 1]^T, ξ_2=[0.5782 - 0.1245i, -0.1176 - 0.0125i, 0.7976]^T, ξ_3=[0.5782 + 0.1245i, -0.1176 + 0.0125i, 0.7976]^T λ_1= 0.6, λ_2= 0.125 + 0.4737i, λ_3=0.125 - 0.4737i;
1/2/1	$f_1(x)$/ $f_2(y)$/ $f_1(z)$	3×4×5	(-1-2,-1), (-1,-1,-1), ..., (1,1,1), (1,2,1)	ξ_1=[0, 0, 1]^T, ξ_2=[-0.2862 + 0.2854i, 0.1371 - 0.0285i, -0.9039]^T, ξ_3=[-0.2862 - 0.2854i, 0.1371 + 0.0285i, -0.9039]^T λ_1= 0.4, λ_2=-0.22 + 0.2358i, λ_3=-0.22 - 0.2358i;
2/2/2	$f_2(x)$/ $f_1(y)$/ $f_2(z)$	6×5×6	(-3,-2,-3), (-3,-2,-2),..., (0,0,0) ,..., (2,2,2), (2,2,3)	ξ_1=[0, 0, 1]^T, ξ_2=[0.3765 - 0.1432i, -0.0884 - 0.0172i, 0.9108]^T, ξ_3=[0.3765 + 0.1432i, -0.0884 + 0.0172i, 0.9108]^T
…		M×N×L	…	…

Actually, the dynamics of the system is classified via its Lyapunov Exponents (*LEs*). The related detail are given in Table2. Also, the sign of the largest LE_{max} determines the relationship between all small perturbations and the state of the system.

When $A = 1$, $a = 2.5$, $b = 1.8$, $c = 0.8$, $d = 1.5$, $e = 0.6$, $h = 0.4$, $N = M = L = 1$, initial conditions $(0.06, 0.06, 0.06)$, the system generates $4 \times 3 \times 3$ scroll attractors and

TABLE 2. The relationship between system state and Lyapunov exponents.

Lyapunov Exponents	system state
$LE_1, LE_2, LE_3 < 0$	stable
$LE_1 > 0, LE_2 \leq 0, LE_3 < 0$	chaos
$LE_1, LE_2 > 0, LE_3 \leq 0$	hyper chaos

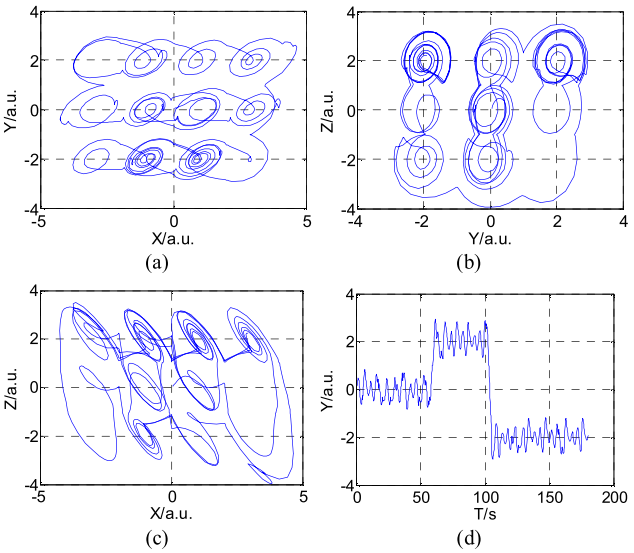

FIGURE 3. 4 × 3 × 3 scroll attractors: (a) x-y; (b) y-z; (c) x-z; (d) y(t).

time domain graph can be shown in Fig.3., the system can be given as follows:

$$\begin{cases} \dfrac{dx}{dt} = -0.6 \times \left[x - \text{sgn}(x) - \text{sgn}(x+2) - \text{sgn}(x-2)\right] \\ \qquad -2.5 \times \left[y - \text{sgn}(y+1) - \text{sgn}(y-1)\right] \\ \dfrac{dy}{dt} = 0.4 \times \left[x - \text{sgn}(x) \text{-sgn}(x+2) - \text{sgn}(x-2)\right] \\ \qquad +1.8 \times \left[y - \text{sgn}(y+1) - \text{sgn}(y-1)\right] \\ \dfrac{dz}{dt} = 1.5 \times \left[x - \text{sgn}(x) \text{-sgn}(x+2) - \text{sgn}(x-2)\right] \\ \qquad -0.8 \times \left[z - \text{sgn}(z+1) - \text{sgn}(z-1)\right] \end{cases} \tag{5}$$

It can be seen from the above figure that when the parameters and initial conditions are set, if a limited range is given, the phase trajectory and time domain conditions can be clearly observed. The *LEs* spectrum is shown in Fig.4.

The *LEs* of system (3) are $LE_1 = 2.17$, $LE_2 = 0$, $LE_3 = -1.01$. Based on the *LEs*, the Hausdroff dimension is also calculated $D_L = 1.39$. Within the time interval, this system shows the chaotic behavior quickly.

III. HOMOCLINIC BIFURCATION AND HETEROLINIC ORBITS

A. THE GEOMETRIC STRUCTURE

Firstly, we extract the essential properties of the vector field associated with system (3) to define a generalized family of vector fields $\boldsymbol{U}$, which is the separatrix plane for each region

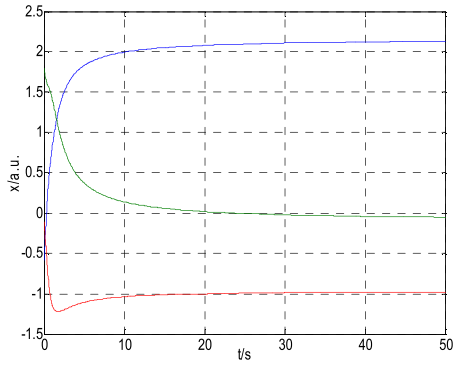

FIGURE 4. Lyapunov exponents spectrum.

but not parallel to each eigenspace and does not through the origin. Let vectors in $\boldsymbol{R^3}$ can be denoted by $X = (x, y, z)^T \in \boldsymbol{R^3}$. Real and imaginary parts of a complex eigenvalue are given by σ and ω, respectively. Real eigenvalues is denoted by γ. Take the direction of scroll attractors is $|x + z| = 1$ as an example, the following conclusion can be obtained.

(i) nonlinear vector fields ($f(x)$) are denoted by S: $\boldsymbol{R^3} \rightarrow \boldsymbol{R^3}$. That means the $S(X)$ can be denoted the vector field evaluated at X and emanating always from the origin P_0, and symmetric with respect to P_0;

(ii) when the system presents three equilibrium points (P_{+1}, P_0, P_{-1}), the planes $\boldsymbol{U}_{\pm 1} = \{(x,z)|(x,z) = \pm 1\}$ are used to define three domains, as shown in Fig. 4:

$$\begin{cases} P_+ = (1, 0, 1) \in D_1 = \{(x, y, z) \,|(x, z) > 1\} \\ P_0 = (0, 0, 0) \in D_0 = \{-1 \le (x, y, z) \,|(x, z) \le 1\} \\ P_- = (-1, 0, -1) \in D_{-1} = \{(x, y, z) \,|(x, z) < -1\} \end{cases} \quad (6)$$

(iii) three equilibrium points, one is located at the origin P_0, one in the interior of D_{+1} (labeled P_+) and the other in the interior of D_{-1} (labeled P_-);

(iv) the eigenspace associated with either the real or the complex eigenvalue at each equilibrium point is not parallel to $\boldsymbol{U_{+1}}$ or $\boldsymbol{U_{-1}}$. For each eigenspace, and define:

$E_c(0) \triangleq 2-D$ eigenspace corresponding to complex eigenvalue at the origin, and the attractor is located in the plane;

$E_r(0) \triangleq 1-D$ eigenspace corresponding to real eigenvalue at the origin;

$E_c(P_+) \triangleq 2-D$ eigenspace corresponding to complex eigen- value at P_+, and the attractor is located in the plane;

$E_r(P_+) \triangleq 1-D$ eigenspace corresponding to real eigenvalue at P_+;

$E_c(P_-) \triangleq 2-D$ eigenspace corresponding to complex eigen- value at P_-, and the attractor is located in the plane;

$E_r(P_-) \triangleq 1-D$ eigenspace corresponding to real eigenvalue at P_-;

$L_0 = E_c(0) \cap U_{+1}$, $L_1 = E_c(P_+) \cap U_{+1}$, $L_2 = \{X \in U_{+1} : S(X)//U_{+1}\}$, $L_3 = E_c(P_+) \cap S_{+1}$, where "// " means "parallel". Here, $S(X)//U_{+1}$ means the vector $S(X)$ lies on a plane parallel to U_{+1}, and L_2 is a straight line in Fig.5. Thus, we have $L_0//L_1$. The saddle focus equilibrium points $P_\pm$ has a real negative eigenvalue whose modulus is large compared with the other eigenvalues, and a pair of complex eigenvalues.

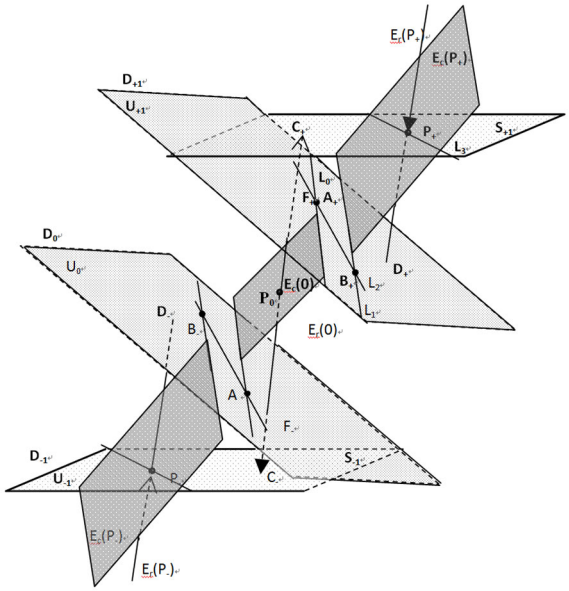

FIGURE 5. Eigenspaces of the equilibria.

In Fig.5, we have defined the following important points: $A_\pm = L_0 \cap L_2$; $B_\pm = L_1 \cap L_2$; $C_\pm = E_r(0) \cap U_{\pm 1} \cap S_{\pm 1}$; $F_\pm = \{X \in L_2\}$ $D_\pm = E_r(P_\pm) \cap U_{\pm 1}$; ; $P_\pm = E_r(P_\pm) \cap S_{\pm 1}$. They can prove that no two lines among L_0, L_1, L_2 , L_3 and L_4 are parallel to each other, except $L_0//L_1$. It is different from the Chua circuit [26]. The existence and significance of relevant important points and straight lines have been proved in [27]. Because of the dual relationship between the Chua system and system (3). We do not need to discuss the common properties between them but the differences via the saddle focus point. Our next goal is to study the possible relationship between the birth (and death) of the attractors and homoclinic bifurcations (homoclinic orbits).

B. HOMOCLINIC ORBIT

According to Shilnikov theorem, it is assumed that there are some homoclinic orbits from P_0 to a saddle focus point. The presence of a saddle-focus separatrix (*i.e.* a homoclinic curve in Poincare's terminology) plays a fundamental role in the onset and disappears of chaotic behavior. To observe this type of trajectory, two conditions should be sufficient: a separatrix loop and Shilnikov's saddle-focus.

The following conditions can be obtained: $a > 1.3$ & $0 < b < e + c$ & $c \ge 0.5$& $e \ge 0.5$& $0 < h < 0.5$, according to the dissipativity and Jacobin matrix of system (3) in order to ensure that a equilibrium point is a hyperbolic saddle focus (or simple, *saddle focus*). Next, some results can be established and proved:

Theorem 1. As a three-dimensional chaotic system, which satisfies the condition $a_{12} \cdot a_{21} < 0$ and can generate multiple scroll attractors at equilibrium points, P_n ($n = 0,1,2,\ldots,N$, N is integer), there are a real eigenvalue $\lambda_3 = \gamma > 0$ and a pair

of complex eigenvalues $\lambda_{1,2} = \sigma \pm i\omega$ with $\sigma < 0, \omega \neq 0$ at each equilibrium. Suppose the following:

(i) The equilibrium point P_0 is a hyperbolic saddle focus;

(ii) At the P_0, the system has a homoclinic orbit H, and if $|\sigma/\gamma| < 1$, the flow can be perturbed into a flow with a countable set of horseshoes.

Proof: Let $p(t) = \{x(t),y(t),z(t)\}$ is the solution of system (3), that

$$\lim_{t\to+\infty} p(t) = p_+ \quad and \quad \lim_{t\to-\infty} p(t) = p_- \tag{7}$$

where $p_+ = p_- = \{p_+, p_-\}$ or $p_+ = p_- = \{p_+, p_0, p_-\}$.

Assume that the system (3) has none of homoclinic orbits joining P_+ and P_-, that is $P_+ \neq P_- \neq P_0$ as $t \in \{+\infty,-\infty\}$.

Denote $p_0 \in R^3$ is the initial point and $p(t; p_0) = \{x(t; p_0), y(t; p_0), z(t; p_0)\}$ is the solution. When $t = 0$, $p(t; p_0) = \{x(t; p_0), y(t; p_0), z(t; p_0)\}$, the following equation can be given

$$\begin{aligned} DL &= \frac{dL\,(x(t), y(t), z(t))}{dt}|_{t=0} \\ &= \left[x(t)\dot{x}(t) + y(t)\dot{y}(t) + z(t)\dot{z}(t)\right]|_{t=0} \\ &= \left[-ex^2\,(t) + by^2(t) - cz^2(t)\right]|_{t=0} \\ &\leq \left[c\left(y^2(t) - z^2(t)\right) - ex^2\,(t)\right]|_{t=0} \\ &\leq \left|c\left(y^2(t) - z^2(t)\right)\right|_{t=0} + \left|ex^2\,(t)\right|_{t=0} \\ &= 0 \end{aligned} \tag{8}$$

When $c \neq 0$ & $e \neq 0$ & $t = 0$, we notice that $DL = 0$. That is $P_+ = P_- = P_0$, it is a contradiction! Therefore, system (3) has the homoclinic orbits. Then, ***Theorem 1*** is proved.

There are three kinds of motion states at each equilibrium, which are the stable state, the critical state and the unstable state. Taking $N = 1$, 3-scroll attractors in x-direction as an example, which is depicted in Fig.6. when the equilibrium point is the saddle focus, the unstable state will evolve into chaos (see ***Theorem 1.***). When $a = 2.2$, $c = 3.1$, $d = 2$, $e = 0$, $h = 1$, by changing the value of b: (1) $b < 0$, the only stable regimes are the equilibrium P_0 (Fig.6.(a) and (b)); (2) as b increases, the equilibrium lost stability at the critical, until $b = 0$, and the periodic orbits appear (Fig.6.(c) and (d)); (3) $b > 0$ increases further, the system undergoes a saddle-node bifurcation, which leads to the appearance of unstable symmetric periodic orbits (Fig.6.(e) and (f)). Therefore, the bifurcation would occur when there are a pair of purely imaginary complex eigenvalues $\lambda_{1,2} = \sigma \pm i\omega$ with $\sigma = 0, \omega \neq 0$ at the origin P_0 in the system (3), that is

$$\lambda_1 + \lambda_2 = 0 \tag{9}$$

This is a only critical condition in combination with a homoclinic bifurcation. Also, $b > 0$ is the bifurcation condition.

Consider changing other parameters, which do not appear to be the chaotic transition like Fig.6. (*i.e.* "stable — critical — unstable", see Fig.7∼12). Because of that the others ($P_\pm$) are not a saddle focus, we don't need to analyze

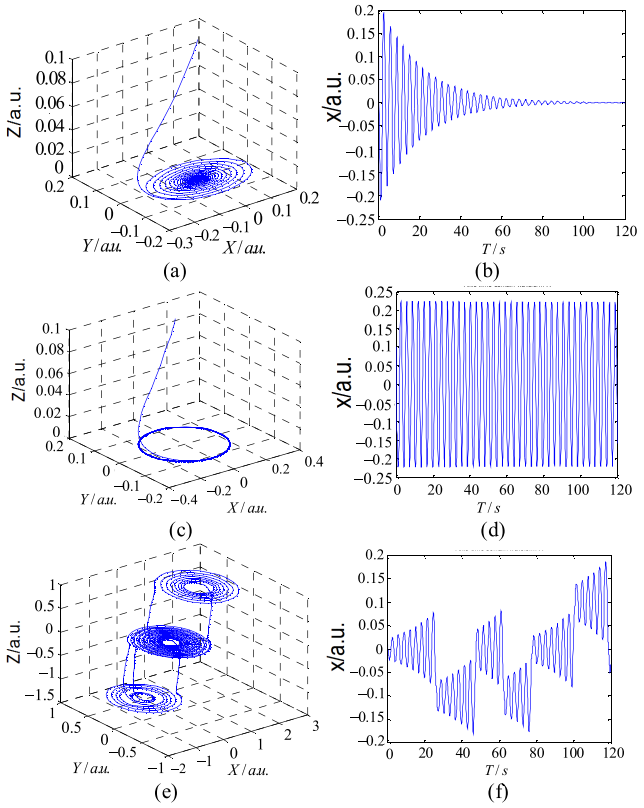

FIGURE 6. Three kinds of motion states: (a) Stable state in 3D, b = −0.1; (b) Stable state in x(t), b = −0.1;(c) Critical state in 3D, b = 0;(d) Critical state in x(t), b = 0; (e) Bifurcation in 3D, b = 0.1; (f) Bifurcation in x(t), b = 0.1.

in detail. According to ***Theorem 1***, the equilibrium P_0 of a vector field is thought a homoclinic point if there exists a trajectory which tends to P_+ as $t \to +\infty$ and as $t \to$-∞ corresponding to the positive engenvalue $\lambda_3 > 0.5$. When the engenvalues $\lambda_{1,2}$ are complex conjugate, the homoclinic trajectory spirals along the eigenplane corresponding to $\lambda_{1,2}$. If there are some parameters to make the trajectory along the unstable real eigenvector from P_0 across the stable eigenspace and return to the origin, and symmetry, it also along the other unstable real eigenvector would behave in the same way. This process is called a homoclinic bifurcation associated with the saddle-focus P_0. Also, this trajectory is called a homoclinic orbit. The existence of a homoclinic orbit is critical to analyze the sensitivity of initial conditions. As a saddle-focus fixed point, the meaning of the *Shilnikov* homoclinic orbit is that a joint of the stable and unstable manifolds, and implies that there is a horseshoe in the neighborhood of this orbit. Therefore, this class of system is chaos.

The simulation (see Fig.6) consistently show that as b increases while fixing other parameters, the scroll attractors collide with each other and eventually emerges after $b > 0$. This collision process leads to the "birth of the scroll attractors". Based on *Shilnikov* Theorem, the keys are to localize the homoclinic orbits in the parameter space and determine the structure of this chaotic system via these orbits. It indicates that the behavior of chaos and bifurcations may

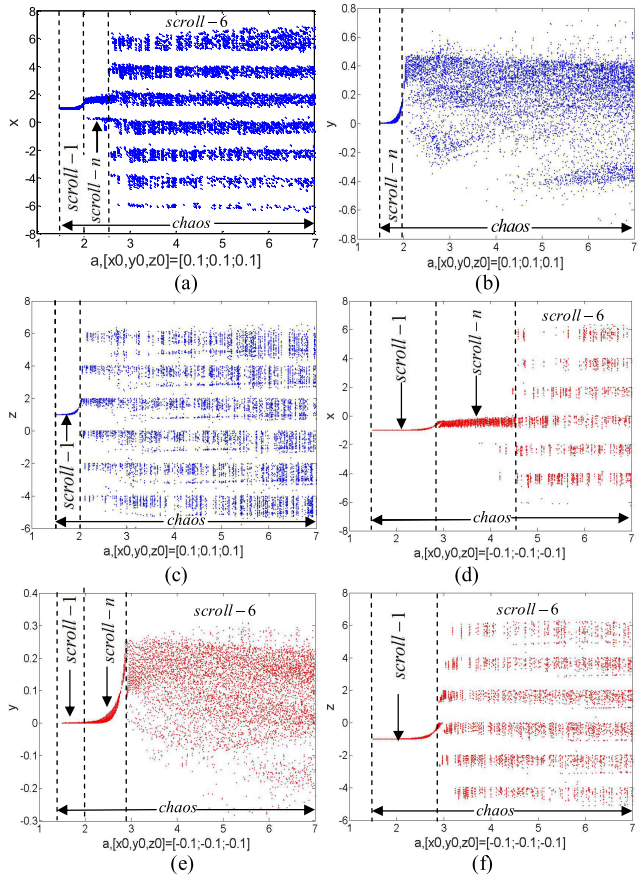

FIGURE 7. Bifurcation diagram showing local maxima of the coordinate versus a: (a) x (t); (b) y (t); (c) z (t); (d) x (t); (e) y (t); (f) z (t).

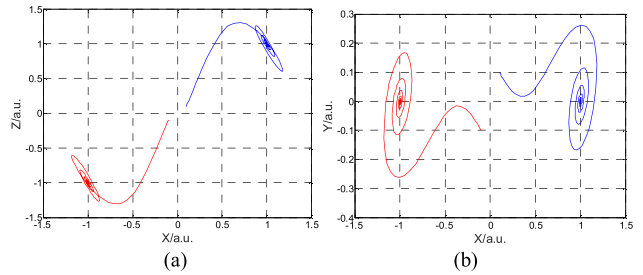

FIGURE 8. The coexisting scroll-1: (a) X-Y; (b) X-Z.

help us to understand the relationship between Shilnikov homoclinic orbits and scroll attractors. However, homoclinic orbits are not structurally stable: they disappear under small perturbations of the vector field. Also, the saddle cycle itself does not undergo any bifurcations.

C. HETEROLINIC ORBIT

The heteroclinic orbit is the other kind of trajectory that could connect an equilibrium point or a closed orbit to another equilibrium point or closed orbit. Also, the existence of them is also assumed in *Shilnikov* theorem. This research is not only a essential but also difficult task for this paper. In this subsection we give a new insight for the existence of this orbit in system (3). Summarizing the above analysis and discussion the following results could be given:

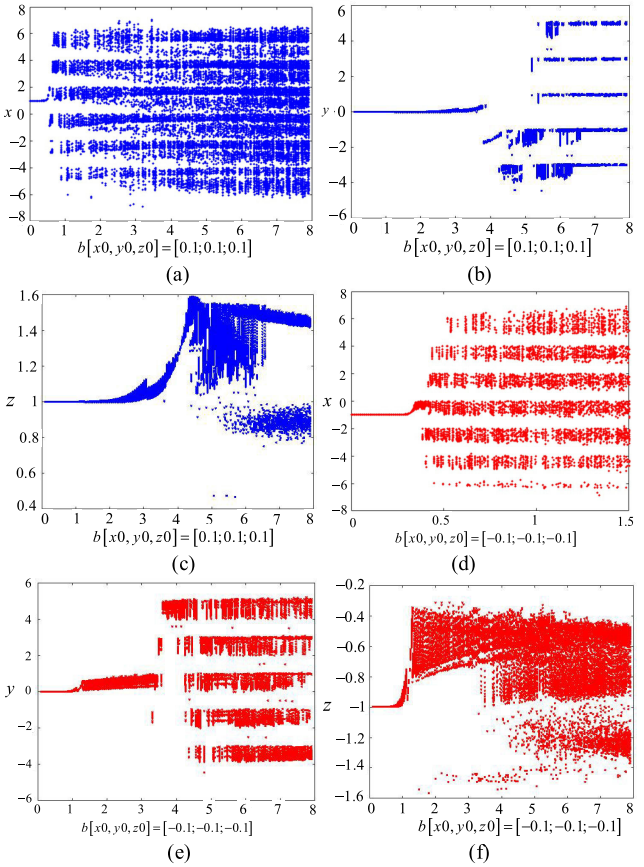

FIGURE 9. Bifurcation diagram showing local maxima of the coordinate versus b: (a) x (t); (b) y (t); (c) z (t); (d) x (t); (e) y (t); (f) z (t).

Theorem 2: As a three-dimensional chaotic system, which satisfies $a_{12}\cdot a_{21} < 0$ and the equilibriums are as in *Theorem 1*. Let P_{2m} and P_{2m+1} ($m = 1, 2, \ldots, N$) be two distinct equilibrium points, which are origin-symmetric. Both P_{2m} and P_{2m+1} are saddle focus that satisfy the *Shilnikov* inequality: $|\gamma_{mi}| > |\sigma_{mi}| > 0$ ($i = 1,2$) with the further constraint $\gamma_{m1}\gamma_{m2} > 0$ or $\sigma_{m1}\sigma_{m2} > 0$. This system exists a heteroclinic loop, H_1, which joins P_{2m} to P_{2m+1} and makes up of two heteroclinic orbits $H_{mi}(i = 1,2)$. Both the system and its perturbed would exhibit the Smale horseshoe chaos.

Proof: Similar *Theorem 1*, there is a function $p(t)$ and assume that the system (3) has none of heteroclinic orbits to joining P_+ and P_-, that is $P_+ = P_- = O$ as $t \to +\infty$ and as $t \to$-∞,and $DL\,|_{t\neq 0} = 0$.

Let $p_+(t) = \{x_+(t),y_+(t),z_+(t)\}$ in $E_C(P_+)$ and $p_-(t) = \{x_-(t), y_-(t), z_-(t)\}$ in $E_C(P_-)$. They are symmetrical to each other. The following equation can be obtained

$$\begin{aligned} DL &= \frac{dL\,(x(t), y(t), z(t))}{dt}|_{t\neq 0} \\ &= x(t)\dot{x}(t) + y(t)\dot{y}(t) + z(t)\dot{z}(t) \\ &= -ex^2\,(t) + by^2(t) - cz^2(t) \\ &\leq \left|c\left(y^2(t) - z^2(t)\right)\right| + \left|ex^2\,(t)\right| \end{aligned} \tag{10}$$

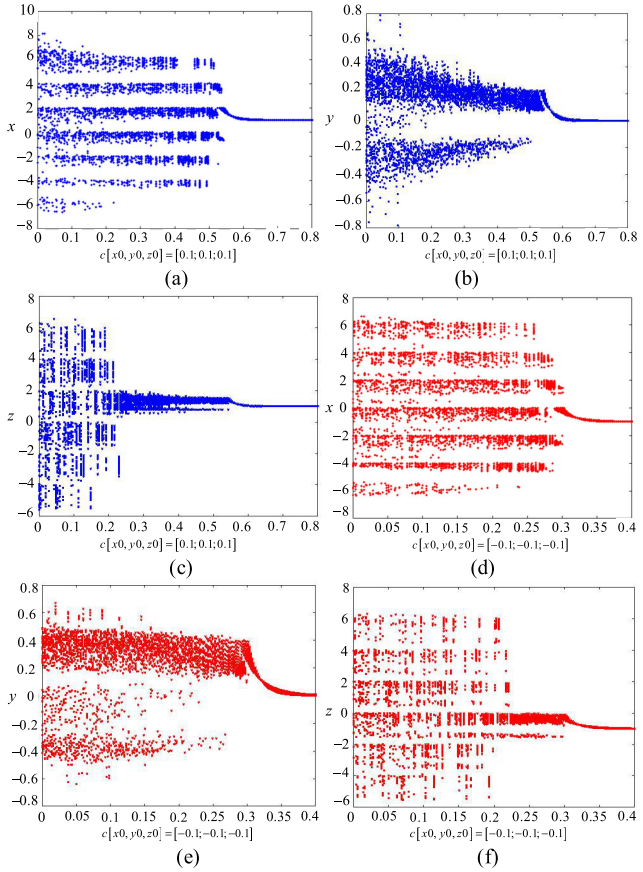

FIGURE 10. Bifurcation diagram showing local maxima of c: (a) x (t); (b) y (t; (c) z (t); (d) x (t); (e) y (t); (f) z (t).

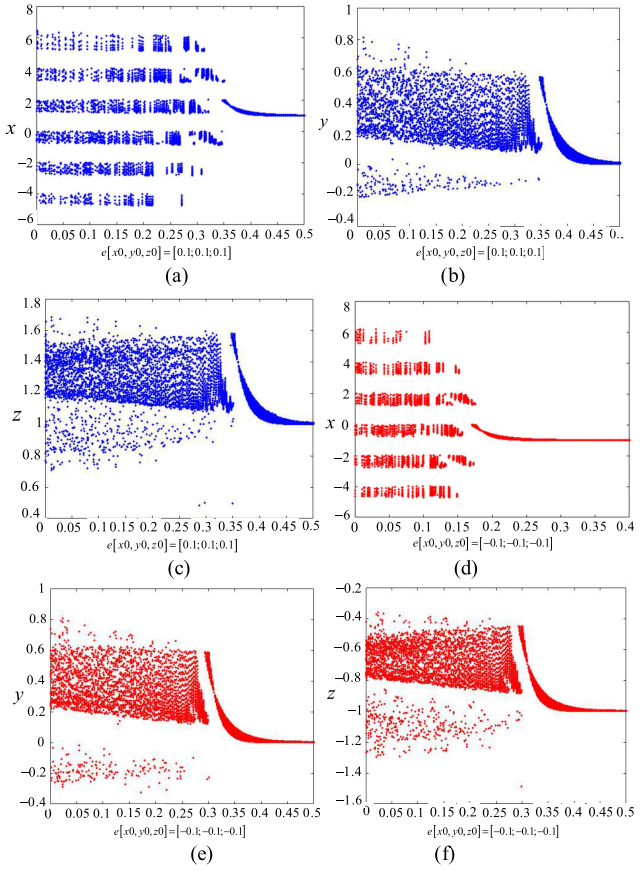

FIGURE 11. Bifurcation diagram of parameter e: (a) x (t); (b) y (t); (c) z (t); (d) x (t); (e) y (t); (f) z (t).

When $c \neq 0$ & $e \neq 0$ & $t \neq 0$, we get $DL \neq 0$ also means $P_+ \neq P_- \neq O$. It is a contradiction! Therefore, there are heteroclinic orbits for system (3). Then, ***Theorem 2*** is thus proved.

According to ***Theorem 2***, we can observe that bifurcation of suitable heteroclinic orbits would get the same features as do bifurcations of homoclinic orbits. It means that a homoclinic orbit is forwards and backwards asymptotic to the same equilibrium P_0, while a heteroclinic orbit is a generalization of a saddle loop.

IV. BIFURCATION AND MULTIPLE SCROLL COEXISTING ATTRACTORS

To investigate the sensitivity of initial condition (x_0, y_0 , z_0) with respect to a single control parameter, we fix A, only vary one parameter in the certain range and setting initial conditions *(0.1, 0.1, 0.1)* (blue solid curve) and *(−0.1, −0.1, −0.1)* (red solid curve), respectively. Bifurcation diagrams can be obtained in Fig.7∼12. Let $M = 3$, $N = 2$, $L = 3$. Case 1: $A = 1$, $b = 0.5$, $c = 0.85$, $e = 0.6$, $h = 0.1$, $d = 1.5$ and $a \epsilon [0,7]$, the bifurcation diagrams are given in Fig.7. Parameters a would be considered in the following:

(1) $a \epsilon$[0,7], blue solid curve

Along with increase of a in the interval [0,0.1581), there is no chaotic behavior and scroll attractors. Then, the orbits from stable to chaos, and to multiple scroll attractors can be observed successively, in the interval [0.1581,7]. Furthermore, three main periodic windows with coexisting scroll-*1* to scroll-*n* ($1 < n < 6$) and to scroll-*6* are obtained, in the intervals [0.581, 2.07), [2.07, 2.585) and [2.585, 7], respectively.

(2) $a \epsilon$[0,7], red solid curve

When a is increasing in the interval [0,0.1581), there is the similar state. Also, in the interval [0.1581,7], the whole movement process can be described from stable to chaos, and to multiple scroll attractors. Three main periodic windows with coexisting are scroll-*1* to scroll-*n* ($1 < n < 6$) and to scroll-*6*, in the intervals [0.581, 2.861), [2.861, 4.498) and [4.498, 7], respectively.

We can also obtain the following results from below bifurcation diagrams: (i) when the initial values and parameters are determined, after a period of time, the final scroll attractors state conforms to the simulation analysis (such as Fig. 2); (ii) with the same conditions but the shorter time, multi-scroll attractors can also be obtained, but the number of number is less than the analysis results, which is not a final state and dangerous. Once it is applied to the engineering, it will lead to the wrong effective or immeasurable losses; (iii) the different number scrolls could be presented and identified hysteretic dynamics (imply multiple stability), which have previously observed in some chaotic system [21], [26].

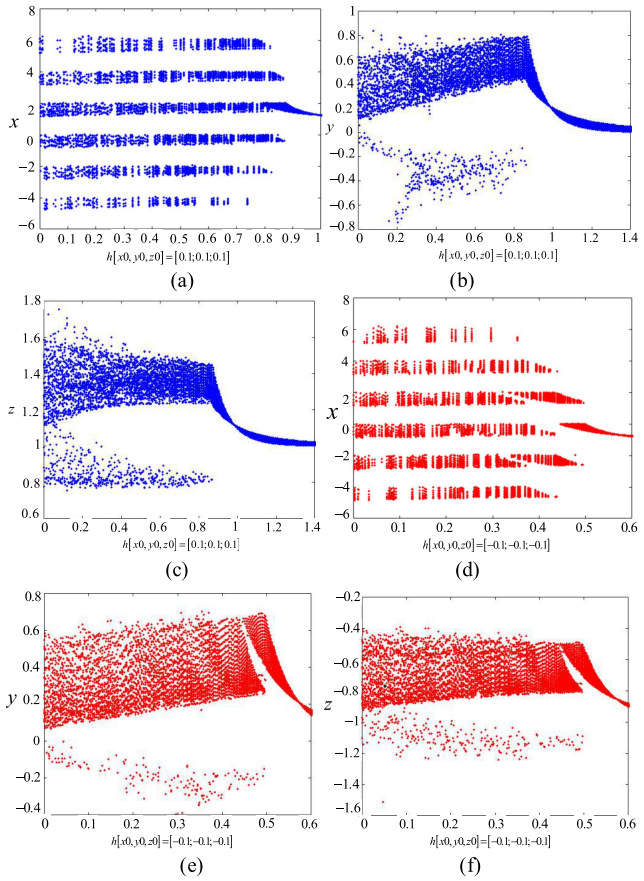

FIGURE 12. Bifurcation diagram of h: (a) x (t); (b) y (t); (c) z (t); (d) x (t); (e) y (t); (f) z (t).

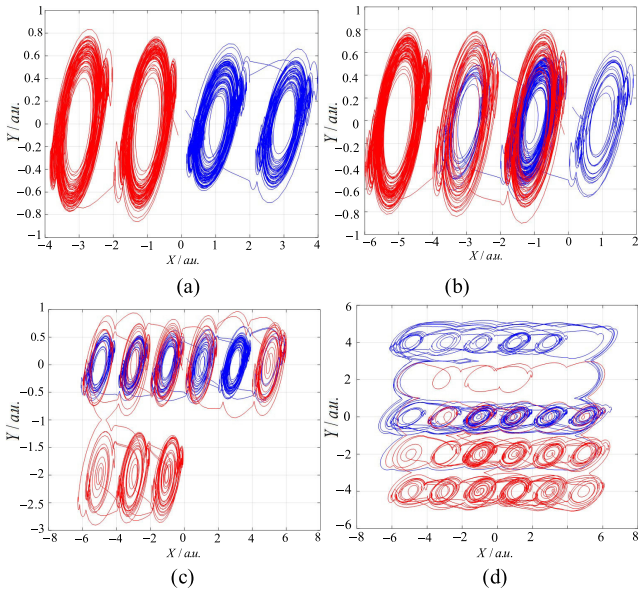

FIGURE 13. The multiple scroll coexisting attractors: (a) a = 2.07 and scroll-2 × 1 × 6; (b) a = 2.074 and scroll-3 × 1 × 6; (c) a = 2.674 and scroll-6 × 2 × 6; (d) a = 2.7 and scroll-6 × 2 × 4.

When $a = 1$, $b = 0.5$, $c = 0.85$, $d = 1.5$, $h = 0.1$, $e = 0.6$, the coexisting scroll-1 attractors are given in Fig.8. Others coexisting scrolls can be shown later (see Fig 13).

It can be seen from above graph that coexisting scroll attractor and the relationship between the number of attractors and initial condition are described clearly. Also, the equilibrium point is also related to the proposed method (*i.e. sign* function) and initial condition, but nothing to do with the parameters.

Case 2: $A = 1$, $a = 3$, $c = 0.85$, $e = 0.6$, $h = 0.1$, $d = 1.5$ when $b \epsilon [0,8]$, the bifurcation diagrams are given in Fig.9:

(1) $b \epsilon [0,8]$, blue solid curve

The orbits occurrence chaotic phenomenon and grid scroll attractors. Three main periodic windows with coexisting are scroll-*1* to scroll-*2* and to scroll-*5*, in the intervals [0,0.5), [0.5, 0.5953) and [0.5953, 8], respectively.

(2) $b \epsilon [0,8]$, red solid curve

Along with increase of b in the interval [0,1.5] by local enlargement, the orbits occurrence chaos and multiple scroll attractors can be observed. Then, three main periodic windows with coexisting scroll-*1* to scroll-*3* and to scroll-*5* can be depicted, in the intervals [0, 0.3344), [0.3344, 0.388) and [0.388, 8], respectively.

Case 3: $A = 1$, $a = 6$, $b = 0.35$, $e = 0.6$, $h = 0.1$, $d = 1.5$ when $c \epsilon [0,0.8]$, the bifurcation diagrams are given in Fig.10. Parameters c will be considered in the following:

(1) $c \epsilon [0,0.8]$, blue solid curve

Three main periodic windows with multiple coexisting are scroll-*6* to scroll-*n* ($1 < n < 6$) and to scroll-*1*, in the intervals [0, 0.5458), [0.5458, 0.5619) and [0.5619, 0.8], respectively.

(2) $c \epsilon [0,0.8]$, red solid curve

when c is increasing in the interval [0,0.4] by local enlargement, three main periodic windows with coexisting are scroll-*6* to scroll-*3* and to scroll-*1*, in the intervals [0, 0.3023), [0.3023, 0.3157) and [0.3157, 0.8], respectively.

Case 4: $A = 1$, $a = 2$, $b = 0.5$, $c = 0.75$, $h = 0.2$, $d = 0.5$ when $e \epsilon [0,0.5]$, the plots are shown in Fig.11.

(1) $e \epsilon [0,0.5]$, blue solid curve

The orbits and attractors would be generated. There are three main periodic windows with coexisting scroll-*6* to scroll-*3* and to scroll-*1*, in the intervals [0, 0.202), [0.202, 0.214) and [0.214, 0.5], respectively.

(2) $e \epsilon [0,0.5]$, red solid curve

The local enlargement can be seen in the interval [0,0.4] Three main periodic windows with coexisting scroll-*6* to scroll-*1* can be observed, in the intervals [0, 0.1753) and [0.1753, 0.4], respectively.

Case 5: $A = 1$, $a = 2$, $b = 0.5$, $c = 0.75$, $e = 0.6$, $d = 0.5$ when $h \epsilon [0,1.4]$, the bifurcation diagrams are depicted in Fig.12. Parameters e will be considered in the following:

(1) $h \epsilon [0, 1]$, blue solid curve

The orbits occurrence chaotic behaviors, multiple scroll attractors and three main periodic windows with coexisting scroll-*6* to scroll-*5* to scroll-*3* and to scroll-*1* are described in the intervals [0, 0.7391), [0.9731, 0.8227), [0.8227, 0.8662) and [0.8662,1], respectively.

(2) $h \epsilon [0,1]$, red solid curve

When h in the interval [0,0.6], we can observe two main periodic windows.

From bifurcation diagrams [see Fig.7(*b,e*), Fig.9(*c, f*), Fig.10(*c, f*), Fig.11(*b, c, e, f*), and Fig.12(*b, c, e, f*)], we further analysis carried out above could occur different number scrolls and identify hysteretic dynamics (imply multiple stability), when monitoring five parameters. In this paper, when parameters of system (3) within a certain range, the long term behavior depends crucially on initial conditions (x_0, y_0, z_0) and parameters. Thus, the interesting and complex dynamics behavior of chaotic attractors can be clearly demonstrated. It ought to be mentioned that, the phenomena of multiple stability have previously observed in Chua system, Jerk circuit, Lorenz-like system [27], *etc*. These systems are also applied in many engineering fields [28]. However, few research on multiple scroll chaotic system before, except [21].

Next, when the parameters (*a, b, c, d, e, h*) = (*a, 0.5, 0.85, 1.5, 0.6, 0.1*), the multiple scroll coexisting attractors are list in Fig.13. It can be seen that the distribution of scroll attractors in below diagram completely conform to the description of the bifurcation plots in Fig.7.

It is well known that as one of the most fundamental bifurcation processes and applications in nonlinear systems, periodic orbits for a chaotic systems can be created and annihilated, this phenomenon can be named antimonoto- nicity [21]. It has been observed in many chaotic system, *i.e.* Jerk circuits, Chua system, Lorenz-like system, and so on. In this paper, it is necessary to form periodic islands in the parameter space, for developing forward and reversed period-doubling bifurcations (see Fig.7∼12). The system (3) appears the chaotic transition ''stable-critical-unstable'' or ''unstable-critical-stable''. A stable symmetric periodic orbit possible around each equilibrium (*i.e.* $P+$ and $P-$) and persist in a certain (rather small and unstable) interval corresponding to the ''periodic-n window''. That means when the parameters vary in a certain range, some discrete values and scrolls can be obtained. Also, antimonotonicity and reverse period-doubling scenarios can occur [11].

According to the above analysis on the Chua system's dual system, we find that it has more complexity than other systems (no matter that the three-dimensional first-order or second-order differential equations.). It means that this type of system has wide potential application value, for example, the memristive system, chaotic secure communication and synchronization control, image encryption algorithm and so on, which are the focus of our next step, including the entropy.

V. CONCLUSION

The research on analysis and application for Chua system ($a_{12}\cdot a_{21}>0$) seem to have reached their maturity. However, as a dual chaotic system and a special canonical model, these studies have been neglected to the system (3), which satisfies $a_{12}\cdot a_{21}< 0$ and has similar but topologically not equivalent dynamic characteristics. Therefore, it is important to supplement them. Also, in most nonlinear dynamical systems, although the rich and interesting varieties of chaotic phenomena can be observed and convincing from computer simulations. It is remain necessary to find a rigorous mathematical method to prove them in order to deal with the legitimate objections from their critics. By exploiting classical nonlinear analysis tools such as *Silinkov* theorem, the saddle focus point, bifurcation diagrams, *LEs*, and phase space trajectories, the existence of chaotic behaviors and dynamics of proposed system has been characterized with respect to its parameters.

As the major results of this work, a method for generating $M\times N\times L$ grid multiple scroll attractors is proposed, two theorems are demonstrated for the bounded orbits (*i.e.* homoclinic and heteroclinic orbits), bifurcation and multiple scroll are also given. The analyzed chaotic system in this paper represents one of the important three-dimensional nonlinear systems that few reported to date and had been not found in other literature before. Furthermore, a very good agreement is observed between theoretical and simulations and it would play a potential role in chaotic dynamic analysis and some engineering applications of chaos theory in future.

REFERENCES

[1] T. Hikihara, P. Holmes, T. Kambe, and G. Rega, ''Introduction to the focus issue: Fifty years of chaos: Applied and theoretical,'' *Chaos, Interdiscipl. J. Nonlinear Sci.*, vol. 22, no. 4, Dec. 2012, Art. no. 047501.

[2] L. Fortuna, M. Frasca, and A. Rizzo, ''Chaotic pulse position modulation to improve the efficiency of sonar sensors,'' *IEEE Trans. Instrum. Meas.*, vol. 52, no. 6, pp. 1809–1814, Dec. 2003.

[3] S. He, K. Sun, H. Wang, X. Ai, and Y. Xu, ''Design of N-dimensional multi-scroll jerk chaotic system and its performances,'' *J. Appl. Anal. Comput.*, vol. 6, no. 4, pp. 1180–1194, Nov. 2016.

[4] Y. Liu, J. Guan, C. Ma, and S. Guo, ''Generation of 2N + 1-scroll existence in new three-dimensional chaos systems,'' *Chaos, Interdiscipl. J. Nonlinear Sci.*, vol. 26, no. 8, Jun. 2016, Art. no. 084307.

[5] Y. Liu and S. Guo, ''Generation and dynamics analysis of N-scrolls existence in new translation-type chaotic systems,'' *Chaos, Interdiscipl. J. Nonlinear Sci.*, vol. 26, no. 11, Oct. 2016, Art. no. 113114.

[6] D. Younesian and H. Norouzi, ''Chaos prediction in nonlinear viscoelastic plates subjected to subsonic flow and external load using extended Melnikov's method,'' *Nonlinear Dyn.*, vol. 84, no. 3, pp. 1163–1179, Dec. 2015.

[7] L. M. Alonso, ''Nonlinear resonances and multi-stability in simple neural circuits,'' *Chaos, Interdiscipl. J. Nonlinear Sci.*, vol. 27, no. 1, Feb. 2016, Art. no. 013118.

[8] V. Sharma, B. B. Sharma, and R. Nath, ''Nonlinear unknown input sliding mode observer based chaotic system synchronization and message recovery scheme with uncertainty,'' *Chaos, Solitons Fractals*, vol. 96, pp. 51–58, Mar. 2017.

[9] X. Ai, K. Sun, S. He, and H. Wang, ''Design of grid multiscroll chaotic attractors via transformations,'' *Int. J. Bifurcation Chaos*, vol. 25, no. 10, Sep. 2015, Art. no. 1530027.

[10] L. Zhou, C. Wang, and L. Zhou, ''A novel no-equilibrium hyperchaotic multi-wing system via introducing memristor,'' *Int. J. Circuit Theory Appl.*, vol. 46, no. 1, pp. 84–98, Mar. 2017.

[11] J. Kengne, A. N. Negou, and D. Tchiotsop, ''Antimonotonicity, chaos and multiple attractors in a novel autonomous memristor-based jerk circuit,'' *Nonlinear Dyn.*, vol. 88, no. 4, pp. 2589–2608, Feb. 2017.

[12] J. Kengne, Z. T. Njitacke, and H. B. Fotsin, ''Dynamical analysis of a simple autonomous jerk system with multiple attractors,'' *Nonlinear Dyn.*, vol. 83, nos. 1–2, pp. 751–765, Sep. 2016.

[13] K. Rajagopal, J. R. Mboupda Pone, S. T. Kingni, S. Arun, and A. Karthikeyan, ''Analysis and electronic implementation of an absolute memristor autonomous Van Der Pol-duffing circuit,'' *Eur. Phys. J. Special Topics*, vol. 228, no. 10, pp. 2287–2299, Oct. 2019.

[14] L. Zhou, C. Wang, X. Zhang, and W. Yao, ''Various attractors, coexisting attractors and antimonotonicity in a simple fourth-order memristive twin-T oscillator,'' *Int. J. Bifurcation Chaos*, vol. 28, no. 4, Oct. 2018, Art. no. 1850050.

[15] B. Bao, F. Hu, M. Chen, Q. Xu, and Y. Yu, "Self-excited and hidden attractors found simultaneously in a modified Chua's circuit," *Int. J. Bifurcation Chaos*, vol. 25, no. 5, Dec. 2014, Art. no. 1550075.

[16] J. Kengne, Z. T. Njitacke, A. N. Negou, M. F. Tsostop, and H. B. Fotsin, "Coexistence of multiple attractors and crisis route to chaos in a novel chaotic jerk circuit," *Int. J. Bifurcation Chaos*, vol. 26, no. 5, Nov. 2016, Art. no. 1650081.

[17] Q. Lai, T. Nestor, J. Kengne, and X.-W. Zhao, "Coexisting attractors and circuit implementation of a new 4D chaotic system with two equilibria," *Chaos, Solitons Fractals*, vol. 107, no. 1, pp. 92–102, Feb. 2018.

[18] W. Zhou, G. Wang, Y. Shen, F. Yuan, and S. Yu, "Hidden coexisting attractors in a chaotic system without equilibrium point," *Int. J. Bifurcation Chaos*, vol. 28, no. 10, May 2018, Art. no. 1830033.

[19] S. Zhang and Y. Zeng, "A simple jerk-like system without equilibrium: Asymmetric coexisting hidden attractors, bursting oscillation and double full feigenbaum remerging trees," *Chaos, Solitons Fractals*, vol. 120, no. 1, pp. 25–40, Mar. 2019.

[20] M. Chen, M. Sun, B. Bao, H. Wu, Q. Xu, and J. Wang, "Controlling extreme multistability of memristor emulator-based dynamical circuit in flux–charge domain," *Nonlinear Dyn.*, vol. 91, no. 2, pp. 1395–1412, Nov. 2017.

[21] Y. Liu and H. H.-C. Iu, "Antimonotonicity, chaos and multidirectional scroll attractor in autonomous ODEs chaotic system," *IEEE Access*, vol. 8, no. 1, pp. 77171–77178, Apr. 2020.

[22] Q. Lai, P. D. Kamdem Kuate, F. Liu, and H. H.-C. Iu, "An extremely simple chaotic system with infinitely many coexisting attractors," *IEEE Trans. Circuits Syst. II, Exp. Briefs*, vol. 67, no. 6, pp. 1129–1133, Jun. 2020.

[23] Q. Lai, Z. Wan, P. D. Kamdem Kuate, and H. Fotsin, "Coexisting attractors, circuit implementation and synchronization control of a new chaotic system evolved from the simplest memristor chaotic circuit," *Commun. Nonlinear Sci. Numer. Simul.*, vol. 89, Oct. 2020, Art. no. 105341.

[24] Q. Lai, B. Norouzi, and F. Liu, "Dynamic analysis, circuit realization, control design and image encryption application of an extended Lü system with coexisting attractors," *Chaos, Solitons Fractals*, vol. 114, pp. 230–245, Sep. 2018.

[25] E. Y. Xie, C. Li, S. Yu, and J. Lü, "On the cryptanalysis of Fridrich's chaotic image encryption scheme," *Signal Process.*, vol. 132, pp. 150–154, Mar. 2017.

[26] R. O. Medrano-T., M. S. Baptista, and I. L. Caldas, "Shilnikov homoclinic orbit bifurcations in the Chua's circuit," *Chaos, Interdiscipl. J. Nonlinear Sci.*, vol. 16, no. 4, Dec. 2006, Art. no. 043119.

[27] X. Wang, J. Chen, J.-A. Lu, and G. Chen, "A simple yet complex one-parameter family of generalized Lorenz-like systems," *Int. J. Bifurcation Chaos*, vol. 22, no. 5, Oct. 2012, Art. no. 1250116.

[28] Z. Li and J. Tang, "A generalized Padé–Lindstedt–Poincaré method for predicting homoclinic and heteroclinic bifurcations of strongly nonlinear autonomous oscillators," *Nonlinear Dyn.*, vol. 84, no. 3, pp. 1201–1223, Jan. 2016.

[29] S. Yu, J. Lü, X. Yu, and G. Chen, "Design and implementation of grid multiwing hyperchaotic Lorenz system family via switching control and constructing super-heteroclinic loops," *IEEE Trans. Circuits Syst. I, Reg. Papers*, vol. 59, no. 5, pp. 1015–1028, May 2012.

[30] C. Zhang and S. Yu, "Generation of grid multi-scroll chaotic attractors via switching piecewise linear controller," *Phys. Lett. A*, vol. 374, no. 30, pp. 3029–3037, Jul. 2010.

[31] Q. Lai and S. Chen, "Generating multiple chaotic attractors from sprott B system," *Int. J. Bifurcation Chaos*, vol. 26, no. 11, Apr. 2016, Art. no. 1650177.

[32] Q. Lai, A. Akgul, L. Li, G. Xu, and Ü. Çavuşoğlu, "A new chaotic system with multiple attractors: Dynamic analysis, circuit realization and S-box design," *Entropy*, vol. 20, no. 1, Dec. 2018, Art. no. 20010012.

[33] H. Xi, S. Yu, R. Zhang, and L. Xu, "Adaptive impulsive synchronization for a class of fractional-order chaotic and hyper-chaotic systems," *Optik*, vol. 125, no. 9, pp. 2036–2040, May 2014.

[34] H. Wen, S. Yu, and J. Lü, "Breaking an image encryption algorithm based on DNA encoding and spatiotemporal chaos," *Entropy*, vol. 21, no. 3, Mar. 2019, Art. no. 21030246.

[35] B. Xu, G. Wang, H. H.-C. Iu, S. Yu, and F. Yuan, "A memristor–meminductor-based chaotic system with abundant dynamical behaviors," *Nonlinear Dyn.*, vol. 96, no. 1, pp. 765–788, Feb. 2019.

[36] X. Wang, J. Yu, C. Jin, H. H. C. Iu, and S. Yu, "Chaotic oscillator based on memcapacitor and meminductor," *Nonlinear Dyn.*, vol. 96, no. 1, pp. 161–173, Jan. 2019.

[37] Z. Lin, S. Yu, J. Lü, S. Cai, and G. Chen, "Design and ARM-embedded implementation of a chaotic map-based real-time secure video communication system," *IEEE Trans. Circuits Syst. Video Technol.*, vol. 25, no. 7, pp. 1203–1216, Jul. 2015.

[38] P. Chen, S. Yu, X. Zhang, J. He, Z. Lin, C. Li, and J. Lü, "ARM-embedded implementation of a video chaotic secure communication via WAN remote transmission with desirable security and frame rate," *Nonlinear Dyn.*, vol. 86, no. 2, pp. 725–740, Jul. 2016.

[39] Q. Wang, S. Yu, C. Li, J. Lü, X. Fang, C. Guyeux, and J. M. Bahi, "Theoretical design and FPGA-based implementation of higher-dimensional digital chaotic systems," *IEEE Trans. Circuits Syst. I, Reg. Papers*, vol. 63, no. 3, pp. 401–412, Mar. 2016.

[40] S. Chen, S. Yu, J. Lü, G. Chen, and J. He, "Design and FPGA-based realization of a chaotic secure video communication system," *IEEE Trans. Circuits Syst. Video Technol.*, vol. 28, no. 9, pp. 2359–2371, Sep. 2018.

[41] L. Yue and H. H. Iu, "Novel floating and grounded memory interface circuits for constructing MEM-elements and their applications," *IEEE Access*, vol. 8, pp. 114761–114772, Jun. 2020.

YUE LIU (Member, IEEE) received the B.S. degree in electrical and information engineering from Liaoning Shiyou University, Liaoning, China, in 2005, the M.S. degree in automation engineering from Northeast Electric Power University, Jilin, China, in 2009, and the Ph.D. degree from Jilin University, Changchun, China, in 2017.

She joined the School of Electrical and Electronic Engineering, Changchun University of Technology, as a Lecturer, in 2018. From 2019 to 2020, she was a Visiting Scholar with The University of Western Australia, Australia. Her research interests include nonlinear dynamics, memory systems, chaos theory, and chaos control and anti-control. She has authored two books and over 20 articles in these areas.

HERBERT HO-CHING IU (Senior Member, IEEE) received the B.Eng. degree (Hons.) in electrical and electronic engineering from The University of Hong Kong, Hong Kong, in 1997, and the Ph.D. degree from The Hong Kong Polytechnic University, Hong Kong, in 2000.

He joined the School of Electrical, Electronic and Computer Engineering, The University of Western Australia, as a Lecturer, in 2002, where he is currently a Professor. His research interests include power electronics, renewable energy, nonlinear dynamics, current sensing techniques, and memristive systems. He has authored over 100 articles in these areas. He is a coauthor of *Development of Memristor Based Circuits* (World Scientific, 2013). He has received two IET Premium Awards in 2012 and 2014, the Vice-Chancellor's Mid-Career Research Award in 2014, and the IEEE PES Chapter Outstanding Engineer in 2015. He currently serves as an Associate Editor for the IEEE TRANSACTIONS ON CIRCUITS AND SYSTEMS II, the IEEE TRANSACTIONS ON POWER ELECTRONICS, IEEE ACCESS, *IEEE Circuits and Systems Magazine*, *IET Power Electronics*, and the *International Journal of Bifurcation and Chaos*. He also serves as an Editorial Board Member for the IEEE JOURNAL OF EMERGING AND SELECTED TOPICS IN CIRCUITS AND SYSTEMS and the *International Journal of Circuit Theory and Applications*. He is a Co-Editor of the *Control of Chaos in Nonlinear Circuits and Systems* (Singapore: World Scientific, 2009).

HUI LI received the B.S. and M.S. degrees from the Changchun University of Technology, Changchun, China, in 1996 and 2002, respectively, and the Ph.D. degree in earth exploration and information technology from Jilin University, in 2007.

She joined the School of Electrical and Electronic Engineering, Changchun University of Technology, as a Lecturer, in 1996, where she is currently a Professor. From 2015 to 2016, she was a Visiting Scholar with Portland State University to study the electrical engineering. Her research interests include artificial intelligence, automotive electronic control, and control theory and application. She has authored two books and over ten articles in these areas.

XUEFENG ZHANG received the B.S. degree in Changchun, China, in 1996. He joined the School of Electrical and Electronic Engineering, Changchun University of Technology, as an Assistant Researcher, in 2006. His research interests include artificial intelligence and automotive control theory and application. He has authored three books and over ten articles in these areas.